

Novel Farnesol and Geranylgeraniol Analogues: A Potential New Class of Anticancer Agents Directed against Protein Prenylation

Barbara S. Gibbs,[‡] Todd J. Zahn,[†] YongQi Mu,^{†,§} Judith S. Sebolt-Leopold,[‡] and Richard A. Gibbs^{*,†}

Department of Cell Biology, Parke-Davis Pharmaceutical Research, 2800 Plymouth Road, Ann Arbor, Michigan 48105, and Department of Pharmaceutical Sciences, College of Pharmacy and Allied Health Professions, Wayne State University, 528 Shaper Hall, Detroit, Michigan 48202

Received June 4, 1999

Protein farnesyltransferase (FTase), the enzyme responsible for protein farnesylation, has become a key target for the rational design of cancer chemotherapeutic agents. Herein it is shown that certain novel prenyl diphosphate analogues are potent inhibitors of mammalian FTase. Furthermore, the alcohol precursors of two of these compounds are able to block anchorage-independent growth of *ras*-transformed cells. While 3-allylfarnesol inhibits protein farnesylation, 3-vinylfarnesol instead leads to abnormal prenylation of proteins with the 3-vinylfarnesyl group. In a similar manner, 3-allylgeranylgeraniol acts as a highly specific inhibitor of protein geranylgeranylation, while 3-vinylgeranylgeraniol restores protein geranylgeranylation in cells. This study indicates that certain prenyl alcohol analogues can act as prenyltransferase inhibitors *in situ*, via a novel prodrug mechanism. These analogues may prove to be valuable tools for investigating the therapeutic consequences of inhibiting geranylgeranylation relative to farnesylation. Furthermore, the 3-vinyl alcohol analogues can inhibit transformed cell growth through a mechanism not involving prenyltransferase inhibition.

Introduction

The initial evidence that proteins are modified with a mevalonate pathway intermediate was presented scarcely over a decade ago. Preliminary biochemical studies quickly demonstrated that there are three different protein prenylation motifs—farnesylation, geranylgeranylation, and bis-geranylgeranylation.¹ The first modification is carried out by an enzyme, protein farnesyltransferase (FTase), which recognizes the CAAX box (where A = aliphatic and X = Ser or Met) at the carboxyl terminus of the protein substrate and then attaches the farnesyl group from farnesyl diphosphate (FPP, **1a**) to the free sulfhydryl of the cysteine residue (Figure 1). The second, closely related enzyme protein geranylgeranyltransferase I (GGTase I) attaches a geranylgeranyl moiety from geranylgeranyl diphosphate (GGPP, **2a**) to a cysteine in a similar CAAX box, where leucine is the carboxyl terminal residue. The third enzyme, GGTase II, attaches two geranylgeranyl residues to two cysteine residues at the carboxyl terminus of Rab proteins.² Since initial studies have demonstrated that Ras, a key protein in signal transduction, is farnesylated, inhibition of FTase has become the subject of intense research interest. While inhibitors of this enzyme are thought to operate by multiple mechanisms of action, in some tumors they block the action of mutant Ras protein thereby halting the growth of *ras*-transformed cells. FTase inhibitors are therefore being developed as potentially novel anticancer drugs.^{3–5}

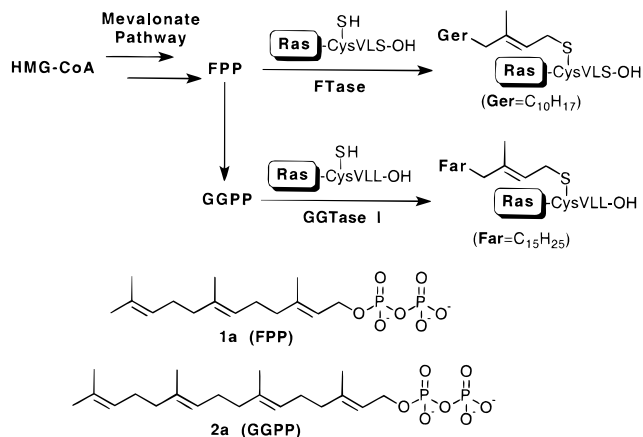


Figure 1. Reactions catalyzed by FTase and GGTase I.

Significant progress has been made in the development of peptide-based FTase inhibitors, and some of these compounds have shown great promise *in vivo* as potential anticancer agents.⁶ However, less work has been done on FPP-based FTase inhibitors, and thus less is known regarding the specificity of FTase for its isoprenoid substrate. We have therefore synthesized novel FPP analogues as probes of the FPP-binding site of FTase and characterized their interaction with recombinant yeast FTase (yFTase). The vinyl analogue 3-vFPP (**1b**, Chart 1) was designed as a potential mechanism-based inhibitor but was instead a poor alternative substrate for yeast FTase.⁷ In contrast, the sterically encumbered analogue 3-tbFPP (**1c**) is an exceptionally poor substrate and a potent competitive inhibitor of this enzyme.⁸ The results seen with 3-tbFPP led us to evaluate it and 3-vFPP against mammalian FTase (mFTase), the clinically relevant variant of the enzyme.

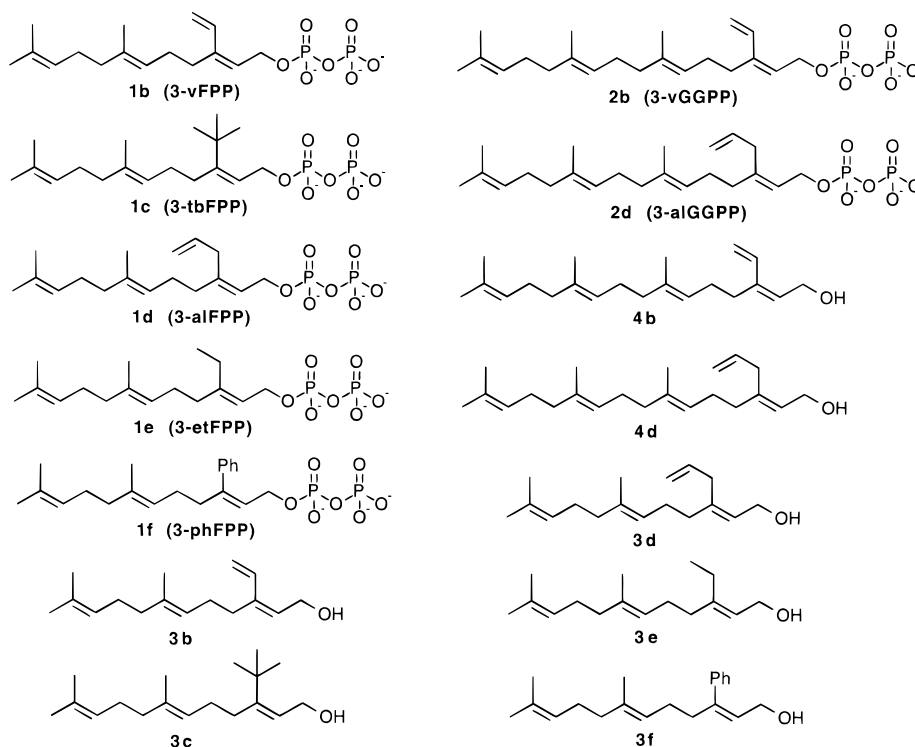
* To whom correspondence should be addressed. Telephone: 313-577-3761. Fax: 313-577-2033. E-mail: rag@wizard.pharm.wayne.edu.

[‡] Parke-Davis Pharmaceutical Research.

[†] Wayne State University.

[§] Current address: Advanced Medicine, 280 Utah Avenue, South San Francisco, CA 94080.

Chart 1

**Table 1.** Inhibition Constants for FPP and GGPP Analogues^a

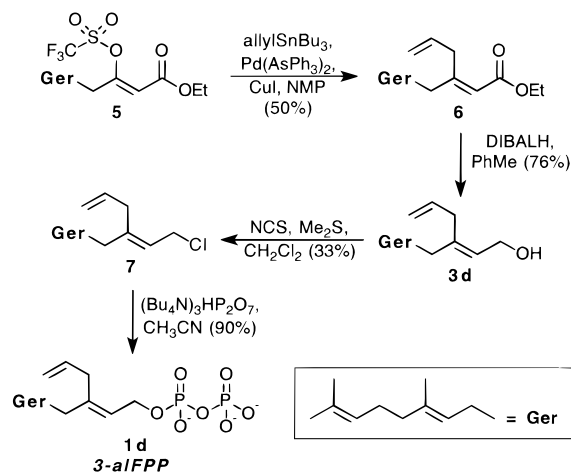
analogue	IC ₅₀	IC ₅₀	K _i	FTase/	K _m	k _{rel}
	FTase	GGTase I	FTase	GGTase	FTase	
3-vFPP	173	~100 000	96 (2700) ^b	~600	156	0.524
3-tbFPP	31	~50 000	8.0 (310) ^b	~1600		
3-alFPP	189	>100 000	31	>530	703	0.0711
3-etFPP	215	>100 000		>460		
3-phFPP	299	>100 000		>340		
3-vGGPP	715	3 050		4.3		
3-alGGPP	453	3 380		7.5		

^a Conditions: All inhibition constants and K_m values are in nanomolar amounts. IC₅₀ and K_i values were determined using recombinant mFTase⁹ or recombinant mGGTase I in a scintillation proximity assay as appropriate (see Experimental Procedures). K_m and k_{rel} (relative V_{max} compared to that obtained with FPP) values were determined using a continuous spectrofluorimetric assay^{20,21} (see Experimental Procedures). Under the conditions of the fluorimetric FTase assay, the K_m determined for FPP itself was 107 nM. ^b Values in parentheses are those previously determined for 3-vFPP⁷ and 3-tbFPP⁸ with yeast FTase.

Results

The mammalian and yeast variants of FTase are quite similar, but they differ sharply in their affinity for the isoprenoid substrate FPP, with mFTase⁹ binding FPP 30-fold more tightly than yFTase.¹⁰ As reported previously, 3-vFPP (**1b**) and 3-tbFPP (**1c**) inhibit yFTase with K_i values of 2.7 μM⁷ and 0.31 μM,⁸ respectively. It is striking, but perhaps not surprising that 3-vFPP and 3-tbFPP are much more potent inhibitors of mFTase than yFTase (Table 1). The selectivity observed for mFTase versus the closely related enzyme mGGTase I is also noteworthy, and is in accord with the 330-fold selectivity that mGGTase I exhibits for its proper isoprenoid GGPP over FPP itself.⁹ These findings prompted us to synthesize three additional 3-substituted FPP analogues: 3-alFPP (**1d**, Scheme 1), 3-etFPP (**1e**, Chart 1), and 3-phFPP (**1f**). All three of these com-

Scheme 1



pounds inhibited mFTase, albeit not as potently as 3-tbFPP. The three most potent inhibitors of mFTase (**1b**, **1c**, and **1d**) were further characterized and were determined to all be competitive inhibitors of the enzyme versus FPP. The increasing interest in GGTase I inhibitors as potential cancer chemotherapeutic agents^{11–14} and our need to evaluate in vivo selectivity (vide infra) prompted us to prepare and evaluate two of the corresponding analogues, 3-vGGPP and 3-alGGPP (**2b** and **2d**, Scheme 2). Surprisingly, both **2b** and **2d** bind more tightly to mFTase than to mammalian GGTase I (Table 1). This underscores the striking difference in diphosphate binding selectivity between these two enzymes that are highly similar in amino acid sequence⁹ and in fact share an identical α subunit.² It also underscores the highly selective nature of GGTase I and the difficulty in obtaining either peptide- or isoprenoid-based inhibitors of this enzyme that do not also inhibit mFTase.¹⁴

Scheme 2

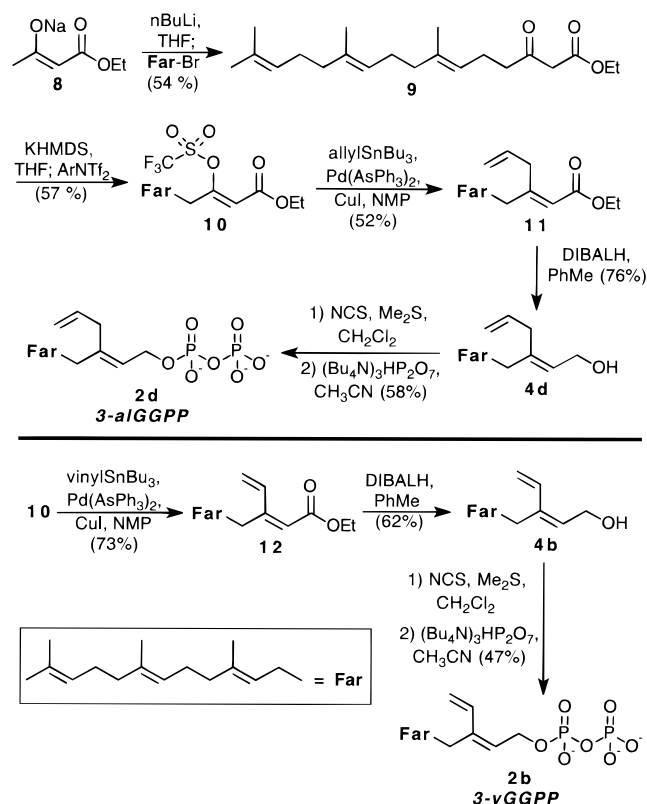


Table 2. Anchorage-Independent Growth Inhibition by Farnesol and Geranylgeraniol Analogues^a

analogue	mean IC ₅₀ (±SE) (μM)	
	H-Ras-F	H-Ras-GG
3-vinylfarnesol (3b)	10.9 ± 2.6 (8)	14.1 ± 1.4 (5)
3-allylfarnesol (3d)	10.2 ± 3.5 (3)	> 25 (4)
3-ethylfarnesol (3e)	> 25 (2)	> 25 (2)
3-phenylfarnesol (3f)	> 25 (2)	> 25 (2)
3-vinylgeranylgeraniol (4b)	18.0 ± 4.1 (5)	13.9 ± 2.3 (4)
3-allylgeranylgeraniol (4d)	> 25 (4)	4.6 ± 1.9 (3)

^a Conditions: Cells were assayed for inhibition of anchorage-independent growth as described under Experimental Procedures. The numbers in parentheses indicate the number of tests performed.

The promising results obtained with these prenyl analogues against mFTase suggested that they should be evaluated as inhibitors of the growth of transformed cells. Unfortunately, isoprenoid diphosphate analogues have poor characteristics as potential drugs, in that they are both unstable and unlikely to penetrate cell membranes unaided, though the natural isoprenoids are apparently taken up by cells through an active transport system.¹⁵ However, it has been demonstrated that mammalian cells can utilize farnesol and geranylgeraniol for the prenylation of proteins.¹⁶ Presumably, the nonpolar alcohols pass through the cell membrane and are then diphosphorylated by a kinase, or sequentially by two kinases, to FPP or GGPP.¹⁷ Therefore, we investigated the ability of the 3-substituted farnesol analogues (**3b–f**, Chart 1) to inhibit the anchorage-independent growth of transformed NIH3T3 fibroblasts in soft agar. Of the four farnesol analogues tested, only the vinyl (**3b**) and allyl (**3d**) compounds exhibited cellular activity (Table 2). 3-*tert*-Butylfarnesol (**3c**) also proved to be inactive in cells (data not shown), which

may be due to the inability of the putative kinase to accept the bulky *tert*-butyl-substituted alcohol. The selectivity of the biologically active compounds was addressed by comparing their relative degree of activity, and that of their geranylgeraniol analogues (**4b** and **4d**, Chart 1), against an isogenic set of transformed cell lines, comprised of NIH3T3 fibroblasts transfected with either H-Ras(61L) [H-Ras-F] or H-Ras(61L)CVLL [H-Ras-GG].¹⁸ The most striking selectivity was observed for 3-allylgeranylgeraniol (**4d**), which exhibited an IC₅₀ of 4.6 μM against H-Ras-GG cells but was totally ineffective (IC₅₀ > 25 μM) against H-Ras-F cells. Conversely, 3-allylfarnesol exhibited selectivity against H-Ras-F cells relative to H-Ras-GG cells. Upon comparison of the biological activities of the various vinyl analogues, H-Ras-F cells were significantly more susceptible to 3-vinylfarnesol (**3b**) than 3-vinylgeranylgeraniol (**4b**), whereas H-Ras-GG cells were equally inhibited by both compounds.

The soft agar data established farnesol analogues **3b** and **3d** as potent inhibitors of soft agar colony formation. However, the mechanism for this effect has not been firmly established. Preliminary data indicating that *raf*-transfected cells are also susceptible to treatment with the vinyl prenyl alcohols suggests that inhibitor of Ras prenylation may not be the sole or primary mechanism of action for these compounds (data not shown). Studies are in progress to investigate the effects of these compounds on normal cell growth, the growth of cultured human cancer cells, and their therapeutic efficacy *in vivo*. To further explore whether the inhibitory actions of the vinyl analogues are due to abnormal prenylation, a series of subcellular fractionation experiments were carried out.¹⁹ H-Ras-F cells were treated with lovastatin in order to block the mevalonate pathway, thereby inhibiting protein prenylation by preventing the formation of FPP and GGPP. This inhibition is evidenced on a Western blot as a shift of the majority of H-Ras from the membrane fraction (DMSO control cells) to the cytosol (lovastatin-treated cells) (Figure 2a). Subsequent treatment of the cells with FPP significantly reversed this effect. Dosing of the lovastatin-treated cells with 3-*al*FPP results in virtually all of the H-Ras being found in the cytosol. This is consistent with 3-*al*FPP acting as an FTase inhibitor rather than a substrate. In sharp contrast, dosing of the lovastatin-treated cells with 3-*v*FPP results in virtually complete localization of the H-Ras protein in the *membrane* fraction. Thus it appears that 3-*v*FPP acts as an *alternative substrate* for FTase, leading to the formation of 3-vinylfarnesylated Ras. As the scintillation proximity assay used initially to evaluate 3-*v*FPP and 3-*al*FPP could not provide evidence for their ability to act as mFTase substrates, these analogues were tested as alternative substrates using a continuous spectrofluorimetric assay.^{20,21} Consistent with the subcellular localization results, 3-*v*FPP is an effective mFTase alternative substrate *in vitro*, and 3-*al*FPP is a very poor one (Table 1). Further confirmation was provided by treatment of H-Ras-F cells with tritium-labeled 3-vinylfarnesol. As shown in Figure 3, the radiolabel migrates with the same protein bands as seen when cells are treated with tritiated farnesol and FPP, verifying the farnesylation of these proteins by 3-*v*FPP.

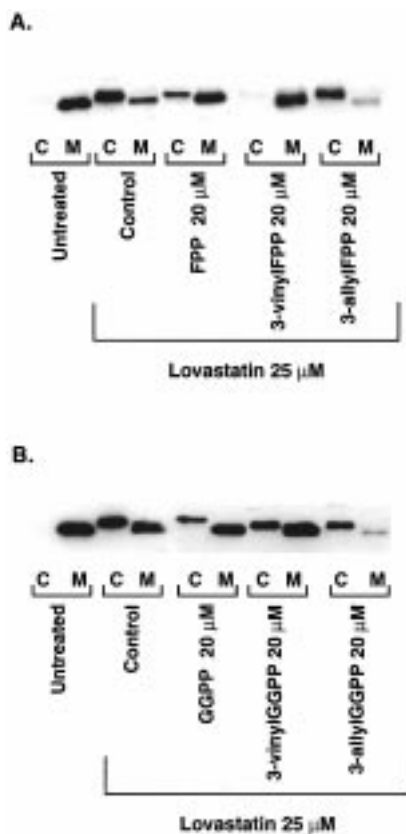


Figure 2. Subcellular fractionation of H-Ras in H-Ras-F and H-Ras-GG cells. H-Ras-F (A) or H-Ras-GG (B) cells were treated with 25 μM lovastatin for 24 h after which the indicated FPP or GGPP analogues (resuspended in media) were added directly to the cell media. Following an additional 24 h incubation period, the cells were harvested and lysed, and the membranes (M) were separated from the cytosol (C).¹⁹ After solubilization of the membrane fraction, Ras protein was immunoprecipitated from both the membrane and cytosolic fractions by the addition of the Y13-259 antibody (OP04 from Oncogene Science).⁴⁰ The presence of Ras protein in each fraction was analyzed by Western blotting (see Experimental Procedures).⁴⁰

However, it appears that the relative levels of radiolabel incorporation into different proteins is not the same with 3-vinylfarnesol as with farnesol itself, although quantitative comparisons cannot be made.

The selectivity and mechanism of the observed cell growth inhibition was further probed through the effects of the 3-vinyl and 3-allyl GGPP analogues on the subcellular distribution of the geranylgeranylated protein variant in H-Ras-GG cells (Figure 2b). With H-Ras-GG cells, as with H-Ras-F cells, blockage of the mevalonate pathway results in a shift in the subcellular location of the Ras protein from the membrane to the cytosol. In accord with the results described above, dosing of lovastatin-treated H-Ras-GG cells with 3-vGGPP, but not 3-alGGPP, results in restoration of the membrane localization of H-Ras-GG. The issue of K-Ras prenylation is of significant interest, as K-Ras is the most commonly found mutant Ras protein in human tumors. Recent studies have demonstrated that K-Ras-transformed cells are more resistant to treatment with FTase inhibitors, which is presumably a result of the ability of the normally farnesylated K-Ras protein to also be geranylgeranylated by GGTase I.¹¹ In accord with this result, dosing of lovastatin-treated, K-*ras*-

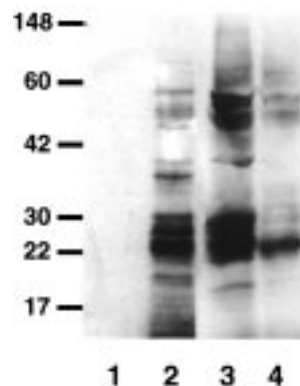


Figure 3. Incorporation of radiolabel into total cellular proteins. H-Ras-F cells were treated with 25 μM lovastatin for 24 h after which the following were added directly to the cell media: (1) untreated, (2) 1-³H-3-vinylfarnesol (5 μM , 1.34 $\mu\text{Ci/mL}$), (3) 1-³H-FPP (3 μM , 50 $\mu\text{Ci/mL}$; Amersham), and (4) 1-³H-farnesol (3 μM , 50 $\mu\text{Ci/mL}$; American Radiolabeled Chemicals). Following an 18 h incubation period, cells were lysed⁴⁰ and proteins separated by SDS-PAGE on a 14% gel and transferred to an Immobilon-P PVDF membrane (Millipore). After drying, the membranes were sprayed with En³-Hance (Amersham) and exposed to film (Hyperfilm MP, Amersham) for 4 days (1-³H-FPP, 1-³H-farnesol) or 28 days (1-³H-3-vinylfarnesol) before developing.

transformed 12V cells with either 3-vFPP or 3-vGGPP results in partial restoration of the membrane localization of K-Ras (data not shown). Preliminary cell proliferation experiments have been performed to characterize the ability of 3-allylfarnesol and 3-allylgeranylgeraniol to block the growth of 12V cells. Surprisingly, both compounds were more effective in blocking the growth of the K-*ras*-transformed 12V cells than the H-*ras*-transformed H61 (H-Ras-F) cell line. After 72 h treatment with 100 μM 3-allylfarnesol, the number of H-Ras-F cells was decreased to $16.6 \pm 4.1\%$ of control, while the number of 12V cells was reduced to $8.6 \pm 1.5\%$ of the control value.

Discussion

In conclusion, our results demonstrate that (a) certain FPP analogues can act as potent inhibitors of mammalian FTase, (b) farnesol and geranylgeraniol analogues can be prodrugs for the corresponding FPP and GGPP derivatives, and (c) these prenyl alcohol derivatives potently inhibit the growth of *ras*-transformed cells. The selectivity of 3-allylfarnesol and 3-allylgeranylgeraniol in soft agar assays (Table 2) and their behavior in the subcellular fractionation experiments (Figure 2) are in accord with previous studies on FTase and GGTase I inhibitors. That is, they appear to block the growth of *ras*-transformed cells by preventing the prenylation of the Ras protein. It is striking and surprising that 3-allylgeranylgeraniol exhibits such selectivity in cells, while 3-alGGPP exhibits no selectivity in vitro (Table 1). Perhaps the intracellular level of GGPP is in the low nanomolar level in contrast to the much higher intracellular FPP concentration.²² If this is true, then 3-alGGPP could compete effectively with the natural substrate for GGTase I but not FTase. Nevertheless, 3-allylgeranylgeraniol is a highly specific cellular inhibitor of protein geranylgeranylation and thus may be a valuable tool to investigate the relative biological importance of geranylgeranylation versus

farnesylation.¹⁴ Recent evidence has suggested that protein geranylgeranylation, and not farnesylation, plays an important role in regulation of endothelial NO synthase and in cell cycle regulation.^{23,24}

In sharp contrast, 3-vinylfarnesol is converted to 3-vFPP, which acts as an alternative substrate for FTase and serves as a prenyl donor both in vitro and apparently in vivo. The corresponding geranylgeranyl analogue 3-vGGPP appears to act in the same manner. Thus the observed biological activity of these compounds is not due to FTase or GGTase I inhibition. It could be due to inhibition of squalene synthase, *cis*-prenyltransferase, or *trans*-prenyltransferase, which utilize FPP to make cholesterol, dolichol, and ubiquinone, respectively. However, the lower affinities of these enzymes for FPP ($K_m = 6 \mu\text{M}$ for squalene synthase;²⁵ $K_m = 24 \mu\text{M}$ for *cis*-prenyltransferase²⁶) make it less likely that micromolar levels of 3-vinylfarnesol or 3-vinylgeranylgeraniol could effectively block their activity in cell culture. Relatively high concentrations of the natural products farnesol and geranylgeraniol have antiproliferative effects on cultured tumor cells,^{27,28} possibly in part through inhibition of phosphatidylcholine biosynthesis.²⁹ However, in control experiments, 30 μM farnesol exhibited little effect on the proliferation of H-Ras-F cells (data not shown), in contrast to the complete inhibition of growth seen with 3-vinylfarnesol.

Evidence has been presented that the prenyl group plays an active role in mediating protein-protein interactions,³⁰⁻³⁴ although this has been a controversial issue.^{1,35} While there are many potential reasons that the 3-vinyl analogues would inhibit cell growth, including those described above, we suggest that the incorporation of the 3-vinylfarnesyl or 3-vinylgeranylgeranyl group into a prenylated protein may interfere with its interaction with various activator or acceptor proteins.³⁶ It is unlikely that Ras protein prenylation is involved, due to the lack of selectivity between H-Ras-F and H-Ras-GG cells. However, the RhoB protein, which is involved in actin cytoskeleton rearrangement, has been implicated as a key target for farnesyltransferase inhibitors,^{4,33} and its 3-vinylprenylation may lead to growth inhibition. Prendergast and co-workers have demonstrated that treatment of cells with FTase inhibitors leads to a decrease in farnesylated RhoB and an increase in geranylgeranylated RhoB, with a concomitant suppression of RhoB-dependent cell growth, consistent with RhoB-GG possessing decreased growth-stimulatory activity relative to RhoB-F.^{4,33} Alternatively, the 3-vinylprenylation of a "protein X" target,^{3c} such as the prenylated protein tyrosine phosphatases, may be responsible for the observed growth inhibition effects. While this proposal is clearly speculative, it suggests that certain prenyl analogues may interfere with the function of prenylated proteins in a manner distinct from that of traditional FTase inhibitors.

Experimental Procedures

Farnesyl and Geranylgeranyl Analogues. Compounds **1b** and **3b**,⁷ along with **1c** and **3c**,⁸ were prepared as previously described. Since **3b** had not been submitted for analysis previously, it was for this study. Analysis: Calcd for $\text{C}_{16}\text{H}_{26}\text{O}$: C, 81.98%; H, 11.10%. Found: C, 80.63%; H, 10.97%. Since the carbon analysis was off by >1%, we also confirmed the structure of **3b** by HRMS: Calcd for $\text{C}_{16}\text{H}_{26}\text{O}$: 234.1984.

Found: 234.1982. Detailed procedures for the synthesis of **3e** and **3f**, the alcohol precursors to 3-etFPP and 3-phFPP, have been published previously,³⁶ and they were converted into the corresponding pyrophosphates using the general procedure of Poulter and co-workers (vide infra).³⁷ The experimental details for the syntheses of compounds **1d**, **2b**, and **2d** are presented below.

Ethyl 3-Allyl-7,11-dimethyldodeca-2(Z),6(E),10-trienoate (6). Triflate **5** (317 mg; 0.794 mmol),⁷ triphenylarsine (25 mg; 0.082 mmol), bis(benzonitrile)palladium(II)chloride (15.3 mg; 0.039 mmol), and copper iodide (15.3 mg; 0.085 mmol) were all placed in an argon-flushed flask and dissolved in 1.0 mL of NMP (*N*-methylpyrrolidone; anhydrous, 99.5%). Allyltributyltin (534 mg; 0.5 mL; 1.61 mmol) was added dropwise, and the reaction was stirred at 100 °C for ~24 h. The mixture was then taken up in a 1:1 solution of hexanes/EtOAc (100 mL), washed with a 10% KF solution (2 × 30 mL) and water (20 mL), then dried over MgSO_4 , filtered, and concentrated. Purification by flash chromatography using a 98:2 hexanes/EtOAc solvent system yielded 118 mg (50%) of the desired allyl ester **6**. ¹H NMR (300 MHz, CDCl_3): δ 1.21 (t, 3H, $-\text{CH}_2-\text{CH}_3$), 1.53 (2s, 6H, two $-\text{CH}_3$), 1.61 (s, 3H, $-\text{CH}_3$), 1.91–2.04 (m, 8H, $-\text{CH}_2-$), 3.34 (d, 2H, allyl $-\text{CH}_2-$), 4.09 (q, 2H, $-\text{OCH}_2\text{CH}_3$), 5.10 (m, 4H), 5.63 (s, 1H, vinylic $-\text{CH}-$), 5.75 (m, 1H). ¹³C NMR (75.4 MHz, CDCl_3): δ 14.3, 16.0, 17.6, 26.6, 36.7, 37.9, 39.6, 59.6, 116.0, 123.9, 124.8, 128.6, 131.3, 133.7, 135.2, 136.1, 160.6, 166.4.

3-Allyl 7,11-Dimethyldodeca-2(Z),6(E),10-trien-1-ol (3d). Allyl ester **6** (100 mg; 0.343 mmol) was dissolved in toluene (2.4 mL; anhydrous) at -78 °C under an argon atmosphere. Addition of diisobutylaluminum hydride (1.0 M in toluene; 1.5 mL; 9.04 mmol) followed, and the reaction was stirred at -78 °C for 1 h. The reaction was quenched by addition to saturated aqueous potassium sodium tartrate (30 mL), the organic phase was separated, and the aqueous layer was extracted with ethyl acetate (3 × 20 mL). The combined organic layers were then washed with water (10 mL) and NaCl (10 mL), dried over MgSO_4 , filtered, and concentrated. Purification by flash chromatography using a 9:1 hexanes/EtOAc solvent system gave 68 mg (76%) of the desired allyl alcohol **3d** as an oil. ¹H NMR (300 MHz, CDCl_3): δ 1.54 (2s, 6H, two vinylic $-\text{CH}_3$), 1.68 (s, 3H, vinylic CH_3), 1.9–2.05 (m, 8H), 2.83 (d, $J = 6.3$ Hz, 2H, allyl $-\text{CH}_2-$), 4.15 (d, $J = 6.8$ Hz, 2H, $-\text{CH}_2\text{OH}$), 5.0–5.08 (m, 4H), 5.51 (t, $J = 6.8$ Hz, 1H, H_2), 5.77 (m, 1H). ¹³C NMR (75.4 MHz, CDCl_3): δ 16.0, 18.2, 26.0, 27.0, 35.5, 37.4, 40.1, 59.6, 115.9, 124.1, 124.7, 125.0, 131.8, 135.8, 136.5, 141.7. Calcd for $\text{C}_{17}\text{H}_{28}\text{O}$: C, 82.2%; H, 11.4%. Found: C, 81.8%; H, 11.5%.

General Procedure for Preparation of Diphosphates.³⁷ *N*-Chlorosuccinimide (1.2 equiv) was dissolved in CH_2Cl_2 (distilled from CaH_2). The solution was cooled to -30 °C in an acetonitrile/dry ice bath. Methyl sulfide (1.5 equiv) was added dropwise, and the resulting milky white mixture was warmed to 0 °C for 5 min and recooled to -30 °C. A solution of 1 equiv of the alcohol in 1 mL of dichloromethane was added dropwise to the mixture at -30 °C. The reaction was slowly warmed to 0 °C and stirred for an additional hour at that temperature. The resulting clear, colorless solution was stirred at room temperature for 20 min and poured into 10 mL of cold brine solution. The aqueous layer was extracted with 2 × 15 mL of hexanes, and the combined organic layers were washed with 10 mL of cold brine solution and dried (MgSO_4). Concentration afforded the chlorides as colorless or pale yellow oils which were used directly for the next reaction. Tris(tetra-*n*-butylammonium)hydrogen pyrophosphate (2 equiv) was dissolved in 1.0 mL of acetonitrile (distilled from P_2O_5). The mixture was cooled to 0 °C, and 1 equiv of chloride in 0.5 mL of acetonitrile was added dropwise. The reaction was stirred at room temperature for 2 h, and the solvent was removed by rotary evaporation at room temperature. The residue was dissolved in 1–2 mL of ion exchange buffer (1:49 v/v isopropyl alcohol and 25 mM NH_4HCO_3) and was passed through a column containing 3–10 mL cation exchange resin (DOWEX AG 50W-X8, NH_4^+ form). The column was eluted with two column volumes of ion exchange buffer at a flow rate of ~1 mL/min.

The eluent was dried by lyophilization, and a pale yellow solid was obtained. The crude product was dissolved in 1–3 mL of 25 mM NH_4HCO_3 and purified by reversed phase HPLC using a program of 5 min of 100% A followed by a linear gradient of 100% A to 100% B over 30 min (A: 25 mM aqueous NH_4HCO_3 , pH 8.0; B: CH_3CN ; Vydac pH-stable C_8 4.6 mm \times 250 mm column; flow rate: 1.0 mL; UV monitoring at 214 and 254 nm). The fractions were collected, pooled, and dried by lyophilization, and the diphosphates were obtained as white fluffy solids. Due to the hygroscopic and amorphous nature of the diphosphates and the limited amounts available in some cases, these compounds were not characterized by elemental analysis. However, these compounds were always purified by reversed phase HPLC, and their purity and identity were confirmed by analytical reversed phase HPLC, ^1H NMR, ^{31}P NMR, and in some cases quantitative phosphate analysis.²¹

3-Allyl-7,11-dimethyldodeca-2(Z),6(E),10-triene 1-Diphosphate (3-alFPP) (1d). Allyl alcohol **3d** (68 mg; 0.261 mmol) was treated with *N*-chlorosuccinimide (60 mg; 0.42 mmol) and dimethyl sulfide (27 mg; 0.03 mL; 0.45 mmol) in 5.0 mL of CH_2Cl_2 . Following the general procedure for the preparation of chlorides described above, 24 mg (33%) of chloride **7** was obtained as a pale yellow oil that was used directly in the next step. Compound **7** (24 mg, 0.087 mmol) was then treated with tris(tetra-*n*-butylammonium) hydrogen pyrophosphate (365 mg; 0.40 mmol) in 3.0 mL of acetonitrile for 2 h. The resulting material was converted to ammonium form by treatment with 3 mL of resin and 8 mL of ion exchange buffer. Following the general reversed phase HPLC purification procedure described above (retention time of 3-alFPP: 17 min), 32 mg (90%) of 3-alFPP **1d** was obtained as a white fluffy solid. ^1H NMR (300 MHz, D_2O): δ 1.57 (s, 6H), 1.63 (s, 3H), 1.95–2.10 (m, 8H), 2.85 (d, 2H), 4.44 (b, 2H), 5.10–5.33 (m, 4H), 5.50 (t, 1H), 5.8 (complex m, 1H). ^{31}P NMR (121 MHz, D_2O): –5.11, –9.15.

Ethyl 7,11,16-Trimethyl-3-oxohexadeca-6E,10E,14-trienoate 9.³⁸ Monosodium ethyl acetoacetate **8** (3.04 g, 20.0 mmol) was dissolved in 30.0 mL of THF under argon. The solution was cooled to 0 °C and treated with *n*-butyllithium (2.0 M in cyclohexane, 10.6 mL, 21.0 mmol). After 20 min at 0 °C, neat farnesyl bromide (1.98 mL, 2.1 g, 7.3 mmol) was added to the resulting dianion solution, and stirring was continued for additional 30 min. The reaction mixture was poured into a cold saturated solution of potassium hydrogen phosphate (~25 mL) and extracted with ether (3 \times 25 mL). The organic layers were combined, washed with water (20 mL), and dried over MgSO_4 . After purification by flash chromatography (hexanes/ethyl acetate 9:1), 1.33 g (54%) of the product **9** was obtained as a pale yellow oil. ^1H NMR (300 MHz, CDCl_3): δ 1.28 (t, J = 7.0 Hz, 3H), 1.59 (s, 3H), 1.60 (s, 6H), 1.68 (s, 3H), 2.00 (m, 8H), 2.28 (m, 2H), 2.54 (t, J = 7.2 Hz, $\text{C}_4\text{-CH}_2$, 2H), 3.43 (s, 2H), 4.20 (q, J = 7.0 Hz, 2H), 5.08 (m, 3H). ^{13}C NMR (75.4 MHz, CDCl_3): δ 14.11, 15.97, 17.66, 22.14, 25.66, 25.71, 26.52, 27.74, 35.21, 39.67, 43.05, 49.31, 49.39, 61.27, 61.34, 122.04, 124.33, 131.28, 135.07, 136.79, 167.19, 202.61. MS-EI: 334 (M^+).

Ethyl 3-(Trifluoromethylsulfonyloxy)hexadeca-7,11,15-trimethyl-2Z,6E,10E,14-tetraenoate 10.³⁸ In an argon-flushed flask, β -ketoester **9** (700 mg, 2.1 mmol) was dissolved in 6.0 mL of THF. The solution was cooled to –78 °C and potassium bis(trimethylsilyl)amide (KHMDS; 0.5 M in toluene, 2.4 mmol, 4.8 mL) was added dropwise. After 1.5 h, a slurry of 2-[*N,N*-bis(trifluoromethylsulfonyl)amide]-5-chloropyridine (946 mg, 2.4 mmol) in 2.0 mL of THF was added to the resulting enolate solution. The reaction was allowed to warm from –78 °C to room temperature over 3 h. It was then taken up in 30 mL of ether, washed with 10% aqueous citric acid (2 \times 15 mL) and water (20 mL), dried over MgSO_4 , and concentrated. Purification by flash chromatography (20:1 hexanes/ethyl acetate) gave 562 mg (57%) of triflate **10** as a pale yellow oil. ^1H NMR (300 MHz, CDCl_3): δ 1.28 (t, J = 7.2 Hz, 3H), 1.56 (s, 3H), 1.60 (s, 6H), 1.62 (s, 3H), 2.17 (m, 8H), 2.39 (m, 2H), 2.43 (t, J = 7.2 Hz, 2H), 4.25 (q, J = 7.2 Hz, 2H), 5.09 (m, 3H), 5.74 (s, 1H). ^{13}C NMR (75.4 MHz, CDCl_3): δ 14.01, 15.98, 16.04, 17.66, 24.39, 25.68, 26.49, 26.72, 34.58,

39.59, 39.68, 61.23, 112.01, 120.55, 123.76, 124.26, 131.32, 135.27, 138.21, 158.46, 162.47. MS-EI: 464 (M^+). Calcd for $\text{C}_{23}\text{H}_{35}\text{F}_3\text{O}_5\text{S}$: C, 57.5%; H, 7.3%. Found: C, 58.0%; H, 7.5%.

Ethyl 3-Allyl-7,11,15-trimethylhexadeca-2Z,6E,10E,14-tetraenoate 11. In a flame-dried, argon-flushed flask were placed triflate **10** (562 mg, 1.2 mmol), $\text{Pd}(\text{PhCN})_2\text{Cl}_2$ (23 mg, 0.061 mmol), AsPh_3 (38 mg, 0.12 mmol), CuI (23 mg, 0.12 mmol), and 1.5 mL of NMP (99.5%, anhydrous). The flask was heated to 100 °C, and to this mixture was added allyltributyltin (0.76 mL, 2.4 mmol). After 15 h at 100 °C the reaction mixture was cooled, taken up in 100 mL of ethyl acetate, and washed with aqueous KF (3 \times 30 mL). The aqueous layer was back-extracted with ethyl acetate (2 \times 15 mL), and the combined organic layers were dried over MgSO_4 . Concentration followed by purification by flash chromatography (hexanes/ethyl acetate 98:2) gave **11** as a colorless oil (222 mg, 52%). ^1H NMR (300 MHz, CDCl_3): δ 1.25 (t, J = 6.8 Hz, 3H, $-\text{CH}_2\text{-CH}_3$), 1.56 (app s, 9H, three $-\text{CH}_3$), 1.68 (s, 3H, $-\text{CH}_3$), 1.95–2.2 (m, 12H, $-\text{CH}_2-$), 3.42 (d, J = 6.0 Hz, 2H, allyl $-\text{CH}_2-$), 4.14 (q, J = 6.8 Hz, 2H, $-\text{OCH}_2\text{CH}_3$), 5.06 (m, 5H), 5.70 (s, 1H, vinylic $-\text{CH}-$), 5.79 (complex m, 1H).

3-Allyl-7,11,15-trimethylhexadeca-2Z,6E,10E,14-tetraen-1-ol 4d. To the solution of ester **11** (191 mg, 0.53 mmol) in 3.0 mL of toluene was added diisobutyl aluminum hydride (1.0 M solution in toluene, 1.5 mL, 1.5 mmol) under argon at –78 °C. The reaction was stirred at –78 °C for 1 h and warmed to room temperature. The reaction was quenched by adding 30 mL of saturated aqueous potassium sodium tartrate. The aqueous solution was extracted with ethyl acetate (2 \times 20 mL). The combined organic layers were washed with saturated NaCl (2 \times 20 mL) and dried over MgSO_4 . Concentration followed by flash chromatography (hexanes/ethyl acetate = 9:1) afforded alcohol **4d** (128 mg, 76%) as a colorless oil. ^1H NMR (300 MHz, CDCl_3): 1.60 (app s, 9H, three vinylic $-\text{CH}_3$), 1.76 (s, 3H, vinylic CH_3), 1.95–2.1 (m, 12H), 2.83 (d, J = 6.3 Hz, 2H, allyl $-\text{CH}_2-$), 4.15 (d, J = 7.0 Hz, 2H, $-\text{CH}_2\text{OH}$), 5.0–5.08 (m, 5H), 5.50 (t, J = 7.0 Hz, 1H, H_2), 5.75 (complex m, 1H). ^{13}C NMR (75.4 MHz, CDCl_3): δ 16.5, 18.1, 26.0, 26.8, 27.2, 30.9, 35.6, 37.5, 40.1, 59.6, 115.9, 116.7, 124.2, 124.5, 124.9, 125.2, 131.6, 135.4, 135.9, 136.6. Calcd for $\text{C}_{22}\text{H}_{36}\text{O}$: C, 83.5%; H, 11.5%. Found: C, 83.4%; H, 11.7%.

3-Allyl-7,11,15-trimethylhexadeca-2Z,6E,10E,14-tetraene Diphosphate 2d. Allyl alcohol **4d** (78 mg, 0.26 mmol) was treated with *N*-chlorosuccinimide (46 mg, 0.34 mmol) and dimethyl sulfide (0.029 mL, 0.39 mmol) in 3.0 mL of CH_2Cl_2 . Following the general procedure for the preparation of chloride described previously, 62 mg (74%) of the corresponding allyl chloride was obtained as a pale yellow oil that was used directly in the next step. The chloride (62 mg, 0.19 mmol) was treated with tris(tetra-*n*-butylammonium)hydrogen pyrophosphate (350 mg, 0.38 mmol) in 3.0 mL of acetonitrile for 2 h. The resulting material was converted to ammonium form by treatment with 3 mL of resin and 8 mL of ion exchange buffer. Following the general reversed phase HPLC purification procedure described above, 62 mg (64%) of 3-alGGPP **2d** was obtained as a white fluffy solid. ^1H NMR (300 MHz, D_2O): δ 1.5–1.7 (3s, 12H), 1.85–2.10 (m, 12H), 2.85 (b, 2H), 4.45 (b, 2H), 4.95–5.15 (m, 5H), 5.50 (t, 1H), 5.7–5.8 (b, 1H). ^{31}P NMR (121 MHz, D_2O): –5.27, –9.15.

Ethyl 3-Vinyl-7,11,15-trimethylhexadeca-2Z,6E,10E,14-tetraenoate 12. In a flame-dried, argon-flushed flask were placed triflate **16** (180 mg, 0.39 mmol), $\text{Pd}(\text{PhCN})_2\text{Cl}_2$ (7.7 mg, 0.02 mmol), AsPh_3 (24 mg, 0.08 mmol), CuI (7.4 mg, 0.04 mmol), and 0.5 mL of NMP (99.5%, anhydrous). To this mixture was added vinyltributyltin (0.14 mL, 0.46 mmol), and the reaction was stirred for 15 h at room temperature. The reaction was taken up with 100 mL of ethyl acetate and washed with aqueous KF (3 \times 30 mL). The aqueous layer was back-extracted with ethyl acetate (2 \times 15 mL), and the combined organic layers were dried over MgSO_4 . Concentration followed by purification by flash chromatography (hexanes/ethyl acetate 20:1) gave **12** as a colorless oil (98 mg, 73%). The identity, and in particular the stereochemistry, of this ester was confirmed by the similarity of its ^1H NMR spectrum to

the previously prepared 3-vinyl-3-desmethylfarnesyl ester. ¹H NMR (300 MHz, CDCl₃): δ 1.28 (t, *J* = 6.9 Hz, 3H), 1.60 (s, 9H), 1.68 (s, 3H), 1.99–2.06 (m, 8H), 2.21 (m, 2H), 2.37 (m, 2H), 4.20 (q, *J* = 6.9 Hz, 2H), 5.11 (m, 3H), 5.44 (dd, 2H, *J* = 1.2, *J* = 11.1 Hz), 5.62 (d, *J* = 17.7 Hz, 1H), 5.70 (s, 1H), 7.73 (dd, 1H, ³*J* = 11.1, 17.7 Hz). ¹³C NMR (75.4 MHz, CDCl₃): δ 14.30, 15.97, 16.08, 17.69, 25.68, 26.75, 27.46, 33.59, 39.68, 59.84, 117.37, 119.87, 123.01, 124.33, 124.08, 131.29, 133.07, 135.04, 136.30, 154.35, 166.32.

3-Vinyl-7,11,15-trimethylhexadeca-2Z,6E,10E,14-tetraen-1-ol 4b. To the solution of ester **12** (95 mg, 0.28 mmol) in 2.0 mL of toluene was added diisobutyl aluminum hydride (1.0 M solution in toluene, 0.7 mL, 0.7 mmol) under argon at –78 °C. The reaction was stirred at –78 °C for 1 h and warmed to room temperature. The reaction was quenched by adding it to 30 mL of saturated aqueous potassium sodium tartrate. The aqueous solution was extracted with ethyl acetate (2 × 20 mL). The combined organic layers were washed with saturated NaCl (2 × 20 mL) and dried over MgSO₄. Concentration followed by flash chromatography (hexanes/ethyl acetate = 4:1) afforded alcohol **4b** (52 mg, 62%) as a colorless oil. ¹H NMR (300 MHz, CDCl₃): δ 1.60 (s, 9H), 1.69 (s, 3H), 2.00–2.05 (m, 8H), 2.18–2.22 (m, 4H), 4.31 (d, *J* = 6.6 Hz, 2H), 5.12 (m, 3H), 5.19 (d, *J* = 9.6 Hz), 5.33 (d, *J* = 17.4 Hz), 5.59 (t, *J* = 6.6 Hz, 1H), 6.64 (dd, *J* = 10.8, 17.3 Hz). ¹³C NMR (75.4 MHz, CDCl₃): δ 16.01, 17.69, 25.68, 26.62, 26.75, 27.13, 33.28, 39.69, 58.61, 11.34, 123.79, 124.14, 124.37, 127.86, 131.29, 132.15, 135.01, 135.56, 139.44. MS-EI: 302 (M⁺). HRMS: Calcd for C₂₁H₃₄O: 302.2610. Found: 302.2613. Analysis: Calcd for C₂₁H₃₄O: C, 83.4%; H, 11.3%. Found: C, 81.4%; H, 11.3%. Due to the unsatisfactory elemental analysis for **4b**, it was subjected to GC/MS analysis of purity (HP5988A GC/MS, DB5ms column, 100–250 °C at 10 degrees/min), which demonstrated that it was >99% pure (retention time: 13.34 min). A second sample of **4b** that was incubated at 30 °C for 24 h under an air atmosphere was 94.3% pure, by GC/MS analysis.

3-Vinyl-7,11,15-trimethylhexadeca-2Z,6E,10E,14-tetraene diphosphate 2b. Vinyl alcohol **4b** (78 mg, 0.26 mmol) was treated with *N*-chlorosuccinimide (46 mg, 0.34 mmol) and dimethyl sulfide (0.029 mL, 0.39 mmol) in 3.0 mL of CH₂Cl₂. Following the general procedure for the preparation of chloride described previously, 62 mg (74%) of the desired vinyl chloride was obtained as a pale yellow oil that was used directly in the next step. The chloride (62 mg, 0.19 mmol) was then treated with tris(tetra-*n*-butylammonium)hydrogen pyrophosphate (350 mg, 0.38 mmol) in 3.0 mL of acetonitrile for 2 h. The resulting material was converted to ammonium form by treatment with 3 mL of resin and 8 mL of ion exchange buffer. Following the general reversed phase HPLC purification procedure described above, 62 mg (64%) of 3-vGGPP **2b** was obtained as a white fluffy solid. ¹H NMR (300 MHz, D₂O): δ 1.57 (s, 9H), 1.64 (s, 3H), 1.97–2.18 (m, 12H), 4.59 (b, 2H), 5.10–5.33 (m, 5H), 5.62 (b, 1H), 6.74 (dd, *J* = 11.4, 11.1 Hz, 1H). ³¹P NMR (121 MHz, D₂O): –6.72, –9.95.

1-[³H]-3-Vinyl 7,11-dimethyldodeca-2(Z),6(E),10-trien-1-ol. Unlabeled 3-vinylfarnesol **3b** (20 mg; 0.085 mmol) was dissolved in hexanes (1.9 mL; anhydrous) in the dark under an argon atmosphere. Manganese dioxide (110 mg; 1.27 mmol) was added in one portion, and the reaction was stirred at room temperature for 90 min [the reaction was followed by TLC (9:1 hexanes/EtOAc)]. The reaction mixture was filtered through a 2.5 cm silica gel plug, which was then washed with ~5 mL of ether. Concentration afforded 21 mg of the desired aldehyde, which was used directly in the next step without further purification. Note that the aldehyde was stable to storage at –78 °C under argon for 72 h, but was unstable to storage overnight at higher temperatures. ¹H NMR (300 MHz, CDCl₃): δ 1.60 (s, 6H, two vinylic -CH₃), 1.70 (s, 3H, vinylic CH₃), 2.0–2.2 (m, 4H), 2.30 (app q, 2H), 2.45 (app t, 2H), 5.15 (m, 2H), 5.60 (d, *J* = 10.8 Hz, 1H), 5.69 (d, *J* = 17.4 Hz, 1H), 5.93 (d, *J* = 7.8 Hz, 1H, H₂), 7.20 (dd, 1H, *J* = 10.8, 17.4 Hz), 10.2 (d, *J* = 7.8 Hz, 1H, H₁). The crude aldehyde (21 mg) was placed in a 3 mL Ace reaction vial equipped with spin vane. Sodium borotritide (8.3 mCi; 150 mCi/mmol; 0.055 mmol;

American Radiolabeled Chemicals) was added as a solution in methanol (0.30 mL; distilled from Mg). After 4 h at room temperature, ~4 mg of sodium borodeuteride was added to complete the reaction, and stirring was continued overnight. The reaction was quenched by addition of saturated NaCl (1 mL), and then the mixture was extracted with ether (3 × 1 mL). Each fraction of ether was passed through a pipet containing MgSO₄ over glass wool, and the combined ether layers were then concentrated. The oil was then taken up in additional ether (~5 mL) and passed through a second plug of MgSO₄ to remove residual water. Following concentration, 19 mg (89%) of the desired alcohol was obtained as an oil (radiochemical yield of 26% (2.17 mCi; specific activity = 27)). Its identity was confirmed by TLC comparison to the unlabeled material and by conversion to 1-[³H]-3-VFPP **1b** (using the general procedure described above) that exhibited HPLC mobility identical to the unlabeled compound and a proton NMR spectrum similar to it except for the decreased size of the C₁ proton signal due to deuterium incorporation.

Prenyltransferase IC₅₀ and K_i Assays. FTase IC₅₀ values were determined using recombinant mFTase⁹ in a scintillation proximity assay (using streptavidin beads from Amersham) with tritiated FPP (specific activity 15–30 Ci/mmol, final concentration 0.12 μM) and the peptide Biotin-Aha-Thr-Lys-Cys-Val-Ile-Met-OH (final concentration 0.1 μM) as substrates, in the same manner as previously described.³⁹ The K_i values were determined using the same assay system with varying concentrations of tritiated FPP. GGase I values were determined in a similar manner using recombinant mGGase I, tritiated GGPP, and the peptide Biotin-Aha-Thr-Lys-Cys-Val-Ile-Leu-OH in a scintillation proximity assay.

Farnesyltransferase K_m and k_{rel} Assays. The kinetic constants for the FPP analogues were determined following a continuous spectrofluorimetric assay originally developed by Pompliano et al. and modified by Poulter and co-workers.^{20,21} Utilizing dansyl-GCVLS as a peptide substrate, the linear portion of the increase in fluorescence versus time was measured with a Spex FluoroMax2 spectrofluorimeter (excitation wavelength = 350 nm; emission wavelength = 486 nm). The assay components [585 μL of assay buffer (52 mM Tris-HCl, pH 7.0, 5.8 mM DTT, 12 mM MgCl₂, 12 μM ZnCl₂), 75 μL of detergent solution (0.4% *n*-dodecyl-β-D-maltoside in 52 mM Tris-HCl, pH 7.0), 45 μL of dansyl-GCVLS solution (12 μM in 20 mM Tris-HCl, pH 7.0, 10 mM EDTA)] were assembled in a 1.5 mL Eppendorf tube in the order indicated above and were incubated at 30 °C for a period of 5 min. FPP, 3-vFPP, or 3-alfPP (~15 mM stock solution in 25 mM ammonium bicarbonate, pH 7.5; final concentration 0.10 to 5 μM) was added to the assay buffer solution. The reaction was then initiated with mFTase, the resulting solution was immediately pipetted into a 1.0 mL quartz cuvette, and fluorescence was detected using a time-based scan at 30 °C for a period of 300 s. Determination of the velocity was determined by converting the rate of increase in fluorescence intensity (cps/s) to μM/s using the formula that has been described previously.²¹ The fluorescence enhancement value *e* was determined individually using FPP, 3v-FPP, and 3-alfPP as substrates.

Western Analysis. Detection of Ras proteins by Western blotting was performed as previously described from this group⁴⁰ using pan-Ras Ab-2 (Oncogene Science) and an anti-mouse HRP conjugate secondary antibody (Amersham). Blots were developed using ECL techniques (Amersham).

Soft Agar Assays. The H-Ras-F, H-Ras-GG, and raf cell lines have been previously described¹⁹ and were grown in Dulbecco's modified Eagle medium supplemented with 10% calf serum and 1% antibiotic/antimycotic at 37 °C and 10% CO₂. Experiments were carried out in 6-well dishes in a two-layer agar system (0.6% bottom layer and 0.3% top layer). Cells were incorporated into the top layer along with varying concentrations of the compound prepared in ethanol. Compound addition only occurred at the time cells were seeded. Subsequent incubation was at 37 °C with 10% CO₂ for 2 weeks. Colonies were stained with 0.5 mL/well of 1 mg/mL *p*-

iodonitrotetrazolium violet (Sigma) 24 h prior to quantitation by image analysis.

Acknowledgment. This research was supported in part by NIH Grants CA-67292 and CA-78819 (to R.A.G.). T.J.Z. was supported in part by a WSU GRA award. Y.Q.M. was the recipient of a Rumble Fellowship from WSU, and R.A.G. was the recipient of an American Cancer Society Junior Faculty Research Award (JFRA-609). We are grateful for the excellent technical support of R. Gowan, M. Latash, and M. Kirzhner (Parke-Davis).

References

- Zhang, F. L.; Casey, P. J. Protein Prenylation: Molecular Mechanisms and Functional Consequences. *Annu. Rev. Biochem.* **1996**, *65*, 241–269.
- Casey, P. J.; Seabra, M. C. Protein Prenyltransferases. *J. Biol. Chem.* **1996**, *271*, 5289–5292.
- (a) Leonard, D. M. Ras Farnesyltransferase: A New Therapeutic Target. *J. Med. Chem.* **1997**, *40*, 2971–2990. (b) Gibbs, J. B.; Oliff, A. The Potential of Farnesyltransferase Inhibitors as Cancer Chemotherapeutics. *Annu. Rev. Pharmacol. Toxicol.* **1997**, *37*, 143–166. (c) Cox, A. D.; Der, C. J. Farnesyltransferase Inhibitors and Cancer Treatment: Targeting Simply Ras? *Biochim. Biophys. Acta* **1997**, *1333*, F51–F71.
- Du, W.; Lebowitz, P. F.; Prendergast, G. C. Cell Growth Inhibition by Farnesyltransferase Inhibitors Is Mediated by Gain of Geranylgeranylated RhoB. *Mol. Cell. Biol.* **1999**, *19*, 1831–1840.
- Sepp-Lorenzino, L.; Rosen, N. A farnesyl-protein transferase inhibitor induces p21 expression and G1 block in p53 wild-type tumor cells. *J. Biol. Chem.* **1998**, *273*, 20243–20251.
- Kohl, N. E.; Omer, C. A.; Conner, M. W.; Anthony, N. J.; Davide, J. P.; DeSolms, S. J.; Giuliani, E. A.; Gomez, R. P.; Graham, S. L.; Hamilton, K.; Handt, L. K.; Hartman, G. D.; Koblan, K. S.; Kral, A. M.; Miller, P. J.; Mosser, S. D.; O'Neill, T. J.; Rands, E.; Schaber, M. D.; Gibbs, J. B.; Oliff, A. Inhibition of Farnesyltransferase Induces Regression of Mammary and Salivary Carcinomas in ras Transgenic Mice. *Nature (Medicine)* **1995**, *1*, 792–797.
- Gibbs, R. A.; Krishnan, U.; Dolence, J. M.; Poulter, C. D. A Stereoselective Palladium/Copper-Catalyzed Route to Isoprenoids: Synthesis and Biological Evaluation of 13-Methylidenefarnesyl Diphosphate. *J. Org. Chem.* **1995**, *60*, 7821–7829.
- (a) Mu, Y. Q.; Gibbs, R. A.; Eubanks, L. M.; Poulter, C. D. Cuprate Mediated Synthesis and Biological Evaluation of *tert*-Butyl and Cyclopropyl Farnesyl Diphosphate Analogues. *J. Org. Chem.* **1996**, *61*, 8010–8015. In addition to our compounds and other related compounds^{8b} that were designed as FPP-competitive inhibitors, several natural products have been found that are potent FPP-competitive mFTase inhibitors.^{8c} (b) For example, α -(hydroxyfarnesyl)phosphonic acid: Gibbs, J. B.; Pompliano, D. L.; Mosser, S. D.; Rands, E.; Lingham, R. B.; Singh, S. B.; Scolnick, E. M.; Kohl, N. E.; Oliff, A. Selective Inhibition of Farnesyl-Protein Transferase Blocks Ras Processing in Vivo. *J. Biol. Chem.* **1993**, *268*, 7617–7620. (c) For example, the chaetomelic acids: Singh, S. B.; Zink, D. L.; Liesch, J. M.; Goetz, M. A.; Jenking, R. G.; Nallin-Omstead, M.; Silverman, K. C.; Bills, G. F.; Mosley, R. T.; Gibbs, J. B.; Albers-Schonberg, G.; Lingham, R. B. Isolation and Structure of Chaetomelic Acids A and B from *Chaetomella acutisetata*: Farnesyl Pyrophosphate Mimic Inhibitors of Ras Farnesyl-Protein Transferase. *Tetrahedron* **1993**, *49*, 5917–5926.
- Yokoyama, K.; Zimmerman, K.; Scholten, J.; Gelb, M. H. Differential Prenyl Pyrophosphate Binding to Mammalian Protein Geranylgeranyltransferase I and Protein Farnesyltransferase and Its Consequence on the Specificity of Protein Prenylation. *J. Biol. Chem.* **1997**, *272*, 3944–3952.
- Dolence, J. M.; Cassidy, P. B.; Mathis, J. R. Yeast Protein Farnesyltransferase: Steady-State Kinetic Studies of Substrate Binding. *Biochemistry* **1995**, *34*, 16687–16694.
- (a) Rowell, C. A.; Kowalczyk, J. J.; Lewis, M. D.; Garcia, A. M. Direct Demonstration of Geranylgeranylation and Farnesylation of Ki-Ras in Vivo. *J. Biol. Chem.* **1997**, *272*, 14093–14097. (b) Whyte, D. B.; Kirschmeier, P.; Hockenberry, T. N.; Nunez-Oliva, I.; James, L.; Catino, J. J.; Bishop, W. R.; Pai, J.-K. K- and N-Ras Are Geranylgeranylated in Cells Treated with Farnesyl Protein Transferase Inhibitors. *J. Biol. Chem.* **1997**, *272*, 14459–14464.
- Lerner, E. C.; Qian, Y.; Hamilton, A. D.; Sebti, S. M. Disruption of Oncogenic K-Ras4B Processing and Signaling by a Potent Geranylgeranyltransferase I Inhibitor. *J. Biol. Chem.* **1995**, *270*, 26770–26773.
- Macchia, M.; Jannitti, N.; Gervasi, G.; Danesi, R. Geranylgeranyl Diphosphate-Based Inhibitors of Posttranslational Geranylgeranylation of Cellular Proteins. *J. Med. Chem.* **1996**, *39*, 1352–1356.
- For a very recent report of a highly selective peptide-based GGTase I inhibitor, see: Vasudevan, A.; Qian, Y.; Vogt, A.; Blaskovich, M. A.; Ohkanda, J.; Sebti, S. M.; Hamilton, A. D. Disruption of Oncogenic K-Ras4B Processing and Signaling by a Potent Geranylgeranyltransferase I Inhibitor. *J. Med. Chem.* **1999**, *42*, 1333–1340.
- Danesi, R.; McLellan, C. A.; Meyers, C. E. Specific Labeling of Isoprenylated Proteins: Application to Study Inhibitors of the Posttranslational Farnesylation and Geranylgeranylation. *Biochem. Biophys. Res. Commun.* **1995**, *206*, 637–643.
- Crick, D. C.; Andres, D. A.; Waechter, C. J. Novel Salvage Pathway Utilizing Farnesol and Geranylgeraniol for Protein Isoprenylation. *Biochem. Biophys. Res. Commun.* **1997**, *237*, 483–487.
- Bentinger, M.; Grunler, J.; Peterson, E.; Swiezewska, E.; Dallner, G. Phosphorylation of Farnesol in Rat Liver Microsomes: Properties of Farnesol Kinase and Farnesyl Phosphate Kinase. *Arch. Biochem. Biophys.* **1998**, *353*, 191–198.
- Cox, A. D.; Hisaka, M. M.; Buss, J. E.; Der, C. J. Specific Isoprenoid Modification Is Required for Function of Normal, but Not Oncogenic, Ras Protein. *Mol. Cell. Biol.* **1992**, *12*, 2606–2615.
- Cox, A. D.; Solski, P. A.; Jordan, J. D.; Der, C. J. Analysis of Ras Protein Expression in Mammalian Cells. *Methods Enzymol.* **1995**, *255*, 195–220.
- Pompliano, D. L.; Gomez, R. P.; Anthony, N. J. Intramolecular Fluorescence Enhancement: A Continuous Assay of Ras Farnesylation: Protein Transferase. *J. Am. Chem. Soc.* **1992**, *114*, 7945–7946.
- Cassidy, P. B.; Dolence, J. M.; Poulter, C. D. Continuous Fluorescence Assay for Protein Prenyltransferases. *Methods Enzymol.* **1995**, *250*, 30–43.
- Bruenger, E.; Rilling, H. C. Determination of Isopentenyl Diphosphate and Farnesyl Diphosphate in Tissue Samples with a Comment on Secondary Regulation of Polyisoprenoid Biosynthesis. *Anal. Biochem.* **1988**, *173*, 321–327. Note that the only known biological role of GGPP in mammalian cells is as a substrate for GGTase I and GGTase II, and thus it is reasonable to propose that its intracellular levels could be very low.
- Laufs, U.; Liao, J. K. Posttranscriptional Regulation of Endothelial Nitric Oxide Synthase mRNA Stability by Rho GTPase. *J. Biol. Chem.* **1998**, *273*, 24266–24271.
- Sun, J.; Qian, Y.; Chen, Z.; Marfurt, J.; Hamilton, A. D.; Sebti, S. M. The Geranylgeranyltransferase I Inhibitor GGTI-298 Induces Hypophosphorylation of Retinoblastoma and Partner Switching of Cyclin-dependent Kinase Inhibitors. *J. Biol. Chem.* **1999**, *274*, 6930–6934.
- Lindsey, S.; Harwood, H. J., Jr. Inhibition of Mammalian Squalene Synthetase Activity by Zaragozic Acid A is a Result of Competitive Inhibition Followed by Mechanism-based Irreversible Inactivation. *J. Biol. Chem.* **1995**, *270*, 9038–9096.
- Ericsson, J.; Thelin, A.; Chojnacki, T.; Dallner, G. Substrate Specificity of cis-Prenyltransferase in Rat Liver Microsomes. *J. Biol. Chem.* **1992**, *267*, 19730–19735.
- Voziyan, P. A.; Haug, J. S.; Melnykovich, G. Mechanism of Farnesol Cytotoxicity: Further Evidence for the Role of PKC-Dependent Signal Transduction in Farnesol-Induced Apoptotic Cell Death. *Biochem. Biophys. Res. Commun.* **1995**, *212*, 479–486.
- Burke, Y. D.; Stark, M. J.; Roach, S. L.; Sen, S. E.; Crowell, P. L. Inhibition of Pancreatic Cancer Cell Growth by the Dietary Isoprenoids Farnesol and Geraniol. *Lipids* **1997**, *32*, 151–156.
- Miquel, K.; Pardines, A.; Terece, F.; Selmi, S.; Favre, G. Competitive Inhibition of Choline Phosphotransferase by Geranylgeraniol and Farnesol Inhibits Phosphatidylcholine Synthesis and Induces Apoptosis in Human Lung Adenocarcinoma A549 Cells. *J. Biol. Chem.* **1998**, *273*, 26179–26186.
- McGeady, P.; Kuroda, S.; Shimizu, K.; Takai, Y.; Gelb, M. H. The Farnesyl Group of H-Ras Facilitates the Activation of a Soluble Upstream Activator of Mitogen-activated Protein Kinase. *J. Biol. Chem.* **1995**, *270*, 26347–26351.
- Okada, T.; Masuda, T.; Shinkai, M.; Kariya, K.; Kataoka, T. Posttranslational Modification of H-Ras Is Required for Activation of, but Not for Association with, B-Raf. *J. Biol. Chem.* **1996**, *271*, 4671–4678.
- Siddiqui, A. A.; Garland, J. R.; Dalton, M. B.; Sinensky, M. Evidence for a High Affinity, Saturable, Prenylation-dependent p21Ha-ras Binding Site in Plasma Membranes. *J. Biol. Chem.* **1998**, *273*, 3712–3717.
- Lebowitz, P. F.; Casey, P. J.; Prendergast, G. C.; Thissen, J. A. Farnesyltransferase Inhibitors Alter the Prenylation and Growth-stimulating Function of RhoB. *J. Biol. Chem.* **1997**, *272*, 15591–15594.

- (34) Myung, C.-S.; Yasuda, H.; Liu, W. W.; Harden, T. K.; Garrison, J. C. Role of Isoprenoid Lipids on the Heterotrimeric G Protein γ Subunit in Determining Effector Activation. *J. Biol. Chem.* **1999**, *274*, 16595–16603.
- (35) Parish, C. A.; Rando, R. R. Isoprenylation/Methylation of Proteins Enhances Membrane Association by a Hydrophobic Mechanism. *Biochemistry* **1996**, *35*, 8473–8477.
- (36) In this regard, we have recently found in a different system that 3-vinylfarnesylation of the yeast α -factor lipopeptide pheromone significantly alters its biological activity, relative to the native farnesylated α -factor: Dawe, A. L.; Becker, J. M.; Jiang, Y.; Naider, F.; Eumner, J. T.; Mu, Y. Q.; Gibbs, R. A. Novel Modifications to the Farnesyl Moiety of the α -Factor Lipopeptide Pheromone from *Saccharomyces cerevisiae* – a Role for Isoprene Modifications in Ligand Presentation. *Biochemistry* **1997**, *36*, 12036–12044.
- (37) Davisson, V. J.; Woodside, A. B.; Neal, T. R.; Stremmler, K. E.; Muehlbacher, M.; Poulter, C. D. Phosphorylation of Isoprenoid Alcohols. *J. Org. Chem.* **1986**, *51*, 4768–4779.
- (38) For a preliminary report on the synthesis of **9** and **10** via a slightly different method, see: Mu, Y. Q.; Gibbs, R. A. Coupling of Isoprenoid Triflates with Organoboron Nucleophiles: Synthesis of *all-trans*-Geranylgeraniol. *Tetrahedron Lett.* **1995**, *36*, 5669–5672.
- (39) Leonard, D. M.; Shuler, K. R.; Poulter, C. J.; Eaton, S. R.; Sawyer, T. K.; Hodges, J. C.; Su, T. Z.; Scholten, J. D.; Gowan, R. C.; Sebolt-Leopold, J. S.; Doherty, A. M. Structure–Activity Relationships of Cysteine-Lacking Pentapeptide Derivatives That Inhibit ras Farnesyltransferase. *J. Med. Chem.* **1997**, *40*, 192–200.
- (40) Scholten, J. D.; Zimmerman, K.; Oxender, M.; Sebolt-Leopold, J.; Gowan, R.; Leonard, D.; Hupe, D. J. Inhibitors of Farnesyl: Protein Transferase-A Possible Cancer Chemotherapeutic. *Bioorg. Med. Chem.* **1996**, *4*, 1537–1543.

JM9902786